Int J Adv Manuf Technol (2017) 88:643–649
DOI 10.1007/s00170-016-8766-2

ORIGINAL ARTICLE

Analysis of surface errors and subsurface damage in flexible grinding of optical fused silica

X. H. Lin[1] · J. B. Zhang[1] · H. H. Tang[1] · X. Y. Du[1] · Y. B. Guo[2]

Received: 12 December 2015 / Accepted: 11 April 2016 / Published online: 27 April 2016
© Springer-Verlag London 2016

Abstract The surface errors and subsurface damage (SSD) formed during optical fused silica grinding processes have been investigated using the flexible grinding wheel (FGW). Surface errors, including low spatial frequency (LSF) errors, middle spatial frequency (MSF) errors, and high spatial frequency (HSF) errors, and SSD depths are measured. Compared with the rigid grinding wheel (RGW), it is found that the influences of grinding parameters on surface errors and SSD are the same in flexible grinding. However, LSF and HSF errors and SSD depths are obviously decreased and MSF errors are partly controlled. The grinding surface micrographs are also observed, and the surfaces after flexible grinding have less grinding scratches and surface defects. These results indicate that flexible grinding using FGW has high precision and elastic characteristics and can achieve good surface quality of optical fused silica.

Keywords Flexible grinding wheel · Surface errors · Subsurface damage · Optical fused silica

1 Introduction

Hard and brittle materials like glasses, ceramics, and carbides have to be machined by abrasive processes. However, it is still difficult for high precision due to their material characteristic and complex form. Precision grinding is primarily considered as an effective machining method to obtain good surface quality including surface errors and subsurface damage (SSD) [1–4]. As for optical parts, form accuracy and surface roughness called low spatial frequency (LSF) and high spatial frequency (HSF) errors, respectively, are deemed as two of the most vital indicators for surface quality. The LSF and HSF errors directly affect the performance of the optical system, while middle spatial frequency (MSF) errors are neglected. However, as research continues into it, MSF errors can cause small angle scattering and decrease the image contrast of optical parts. Current intense laser systems, like National Ignition Facility (NIF) in the USA and SG-3 in China, have strict requirements for MSF errors [5–7]. SSD affect the threshold damage value of the laser driver strongly and the weak anti-damage ability of optical parts. Moreover, the residual stress released by SSD cause deformation and inferior form accuracy of optical parts. In addition, more machining time will be devoted to eliminating SSD. Therefore, reducing SSD in the grinding process is vitally important for high precision and production efficiency [8].

To reduce the surface errors and SSD in optical part grinding, many researchers focus on the optimization of grinding parameters. Demir et al. investigated the effects of grain size on workpiece surface roughness and grinding forces. The results showed that increasing the grain size and depth of cut increased the grinding forces and surface roughness [9]. Zhou et al. proposed a method for controlling the MSF errors located in a definite area in a large optical surface and correcting errors in the definite area, which had the advantages of determinacy and high efficiency [10]. Tool path planning was applied in grinding or polishing to reduce MSF errors, including Hilbert, Peano, and bi-scanning paths. Great efforts were done, and it turned out path planning can help to suppress

✉ X. H. Lin
xhxmut@163.com

[1] Department of Mechanical and Automotive Engineering, Xiamen University of Technology, Xiamen 361024, China

[2] Department of Mechanical and Electrical Engineering, Xiamen University, Xiamen 361005, China

MSF errors, like Tam and Cheng [11] and Dunn and Walker [12]. The researches on SSD are mostly based on the experiments. Li et al. showed morphology and SSD depths of fused silica on different grinding parameters and then discussed the influence of grinding parameters on SSD depths [13]. In the aspect of relation between surface roughness (SR) and SSD, Gu et al. and Esmaeilzare et al. investigated four modes of grinding and different grinding parameters, respectively [14, 15]. Furthermore, Chen et al. researched the influence of wheel speed and chatter on SR and SSD by theoretical analysis, verified by grinding experiments [16].

Because of its flexible characteristic, it is well known that using the flexible grinding wheel (FGW) can reduce the effect of vibration and contribute to good surface quality. Bzymek et al. designed a grinding wheel with variable hub thicknesses, which help to suppress chatter [17]. A novel non-truing flexible grinding wheel-integrated bonnet, spring ring, and grinding belt was designed for grinding steel. Compared with the resin bond grinding wheel, it obtained better grinding accuracy [18]. Webster and Tricard developed a FGW that included sensors to monitor the grinding process [19]. In addition, a soft abrasive grinding wheel is adopted for high precision grinding. Zhou et al. applied this technology on silicon grinding, and the results showed good surface/subsurface quality [20].

Many works were done on surface errors and SSD in grinding of optical parts. In spite of this, little has been discussed on flexible grinding; even so, they were only focused on LSF errors, not to mention in optical part grinding. In this paper, a novel FGW is designed and experiments were carried out to investigate LSF, MSF, and HSF errors and SSD of optical fused silica. The results indicate that this grinding method can obtain better surface quality.

2 Experimentations

2.1 Design of flexible grinding wheel

FGW is a tool that combines the virtues of both the rigid grinding wheel (RGW) and grinding belt, which is expected to be adopted in a grinder instead of the RGW. FGW consists of a grinding belt, bonnet, rubber layer, flange, wheel body, and so on, as shown in Fig. 1. The pressure of the bonnet can be adjusted in accordance with the machining condition, by which it is not only adopted for adjustment of the FGW's rigidity but also for belt tensioning. To decrease the roundness error of FGW, the rubber layer should be well trued before grinding and counterbalance should be considered.

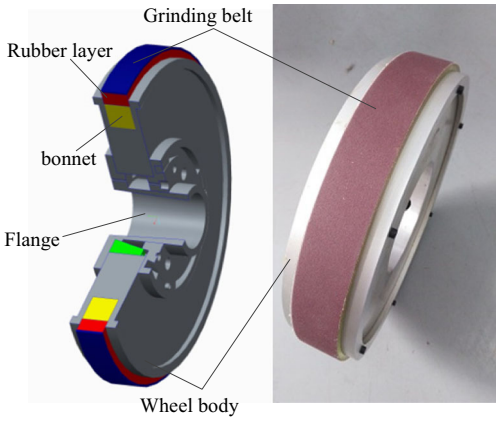

Fig. 1 Structure of FGW

2.2 Flexible grinding of optical fused silica

The precision of a formed grinding wheel is often dependent on truing. A GC-cup truer is applied to true the rubber layer of FGW. Considering the elasticity of the rubber layer and the truing efficiency, two kinds of GC grits of 45# and 120# are applied for rough and fine truing, respectively. The balance weights in the flange can be adjusted for static balance. The SBS 0850L balance system is used for dynamic balance. The laser displacement sensor (KEYENCE LK-G10) is used to measure the roundness error of FGW. By increasing the pressure of the bonnet appropriately, the grinding belt is tensioned along the rubber layer. The grinding experiments are carried out in the precision grinder. The rectangle fused silica samples were clued on a flat iron by hot cement. The surface roughness of samples (Ra) are about 6~8 nm. According to literatures [15, 21], this SSD is minimal relative to the SSD caused by grinding; therefore, it will not affect the experimental results. The RGW is adopted for fused silica grinding by the same parameters for comparative analysis. The grinding parameters are detailed in Table 1.

2.3 Surface error measurement

The surface errors were measured by the Taylor Hobson PGI Dimension 3 Profiler. The measurement parameters are shown in Table 2.

The *X*-axis is defined as the parallel grinding direction while the *Z*-axis is defined as the vertical grinding direction. Two direction profile errors were measured, and the results are shown in Fig. 2.

The surface topography of fused silica was observed by Keyence VHX-2000C microscope, including surface texture and damage. Combining chemistry etching, layer polishing, and laser focus scanning technology, the subsurface damage depths were obtained based on calculation model of SSD. SSD can be predicted accurately via measuring surface

Table 1 Grinding parameters

Grinding parameters		Values
Grit/μm	FGW	24~28
	RGW	15~20
Size (mm × mm)		30 × 30
Wheel speed (rpm)		1500
Feed rate (m min^{-1})		3, 5, 7
Grinding depth (μm)		5, 10, 15, 20, 25

roughness of grinding optical parts. This method is detailed in our review [22] and adopted in this paper.

3 Results and discussions

3.1 Analysis of LSF errors

The surface errors are measured in the size of a 25 × 25 mm area, and five measurement trajectories are planned in each direction with the same intervals to form data grids that are meshed using Matlab [23]. The peak and valley (PV) is an indicator to evaluate the value of LSF errors. As shown in Fig. 3, PV in FGW grinding is 0.17 μm, while PV in RGW grinding is 2.25 μm. Therefore, the LSF errors in FGW grinding are much less than RGW grinding. In addition, the distribution of surface errors is quite different in the two grinding modes. The distribution of surface errors in FGW grinding is relatively average and easier for compensation grinding.

3.2 Analysis of MSF errors

Power spectral density (PSD) is well known as a main evaluated method for criterion of NIF. The range of MSF is divided into two sections: PSD1 (0.03~0.4 mm^{-1}) and PSD2 (0.4~8.3 mm^{-1}). According to the requirement of NIF, the measured PSD curve should be below the criterion curve of NIF. A two-dimensional PSD was calculated for a profile from the measurements of FGW grinding. As shown in Fig. 4a, the PSD curve of FGW is partly above the criterion curve of NIF in the range of MSF errors, which means the MSF errors are not satisfied for PSD2, but PSD1. Compared to RGW grinding, as shown in Fig. 4b, the PSD curve of RGW is all above the criterion curve of NIF, which means the FGW grinding has partly suppressed MSF errors. The reasons are that the elastic characteristic of FGW has an effect on squeezing and polishing on the grinding surface and then the regular ripples caused by convolution and grinder vibration within range of PSD1 are partly eliminated.

Table 2 Measurement parameters (Taylor Hobson)

Measurement parameters	Values
Diamond stylus	*L*, 60 mm; *R*, 2 μm (112-3227-02)
Scan speed (mm s^{-1})	0.25
Sampling interval (μm)	2
Resolution (nm)	0.8

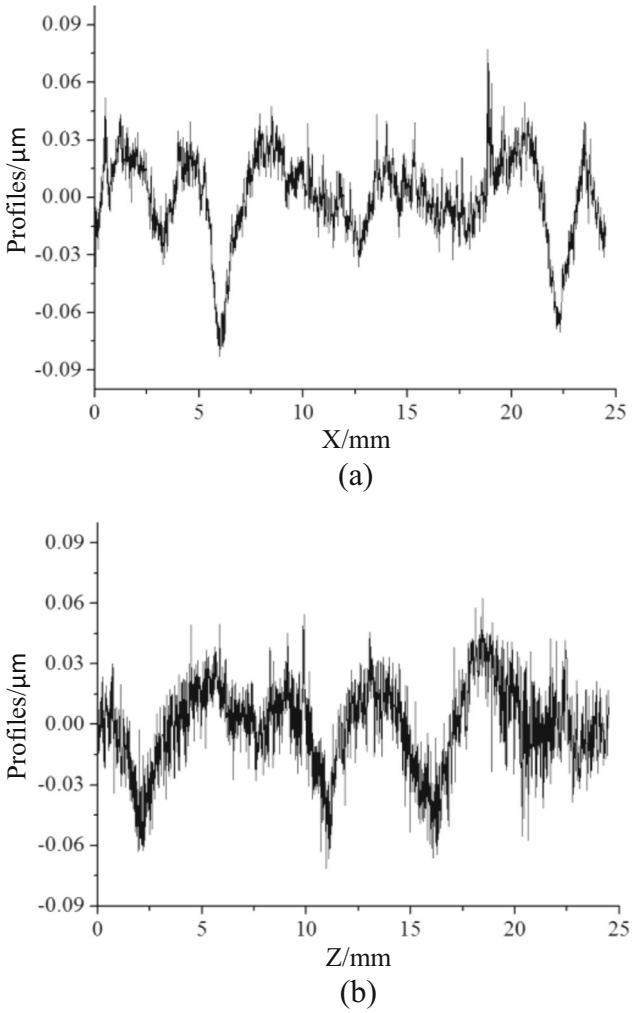

Fig. 2 Profiles errors of two grinding directions in FGW grinding. **a** Parallel grinding direction. **b** Vertical grinding direction

3.3 Analysis of HSF errors

The HSF errors were measured in the parallel and vertical grinding directions. Figure 5 shows the relationship between SR and grinding depth, and Fig. 6 shows the relationship between SR and feed rate in two grinding modes. The values of Ra increase with increasing of the grinding depth/feed rate and the values of Ra in the vertical direction are larger than in the parallel direction. The values of Ra in RGW grinding range from 0.4 to 0.6 μm. By contrast, the values of Ra in

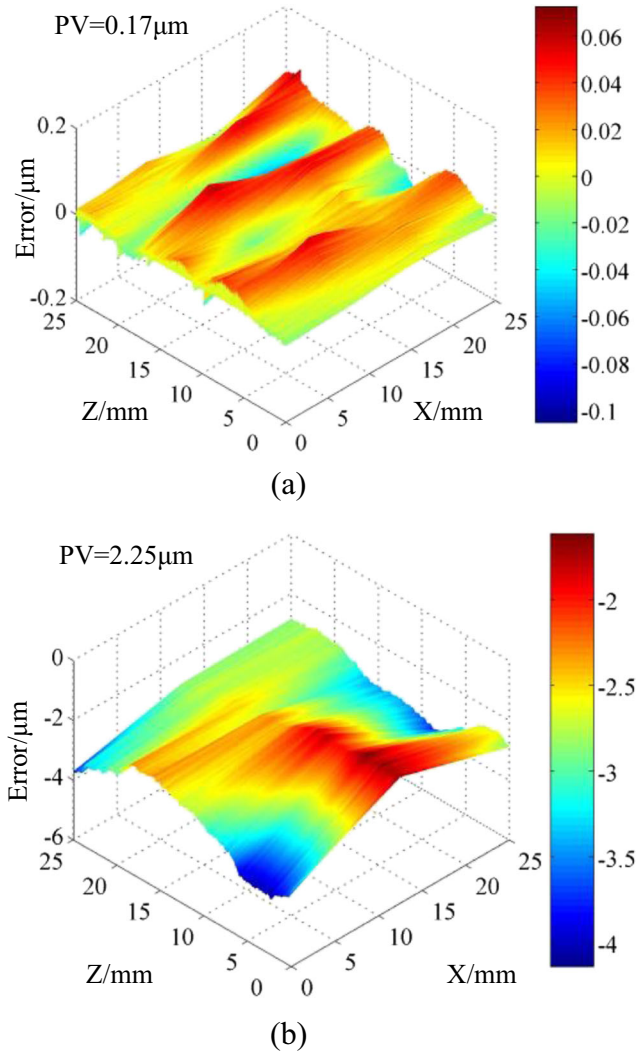

Fig. 3 Distribution of LSF errors. **a** FGW grinding. **b** RGW grinding

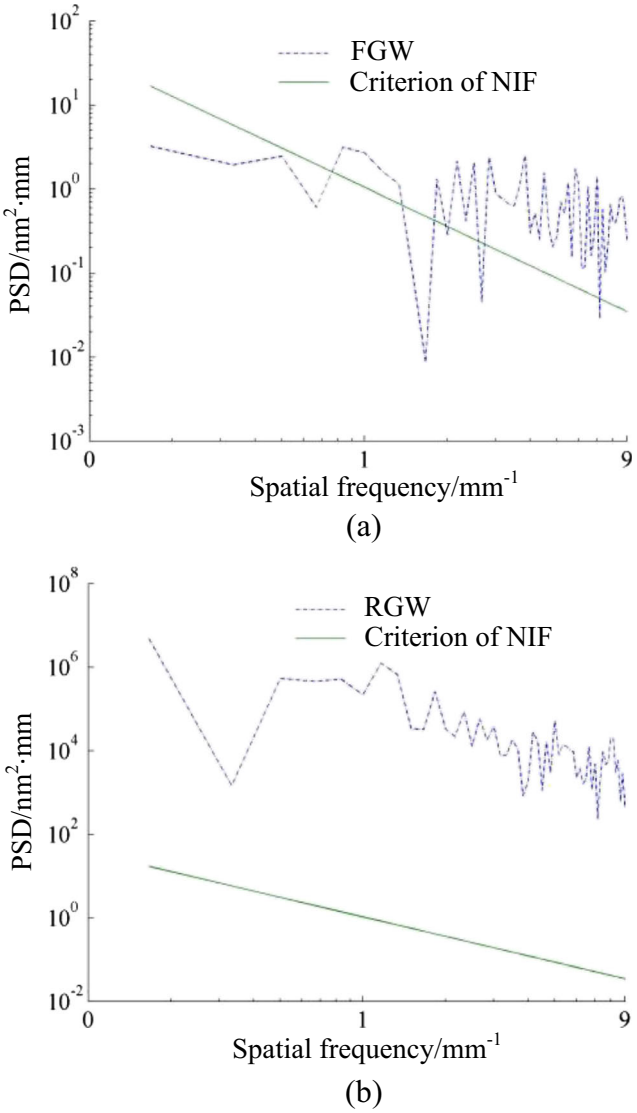

Fig. 4 Comparison of measured and criterion PSD. **a** FGW grinding. **b** RGW grinding

FGW grinding range from 0.01 to 0.04 μm. It is illustrated that FGW grinding has an advantage in obtaining low surface roughness.

Grinding force is a key parameter that affects SR and SSD. In the flexible grinding process, average edge grinding force f_n can be described as follows [24]:

$$f_n = \frac{F_n}{b}\left(\frac{W_e^2}{l_c}\right) \tag{1}$$

Where F_n is the normal grinding force, b is the wheel width, W_e is the average edge gap, and l_c is the contact length.

Although W_e and l_c both increase with decreasing of grinding wheel hardness, the increasing rate of l_c is much more than W_e. Therefore, f_n in flexible grinding is less than diamond grinding. According to the theoretical model proposed by Lambropoulos et al. [25], the grinding grit is considered as a sharp indenter to calculate the median and lateral crack depth. The value of SR is deemed to approximate the

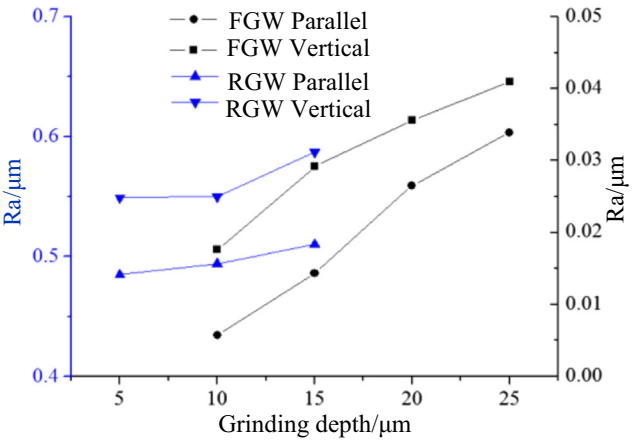

Fig. 5 Variation of SR with respect to grinding depth

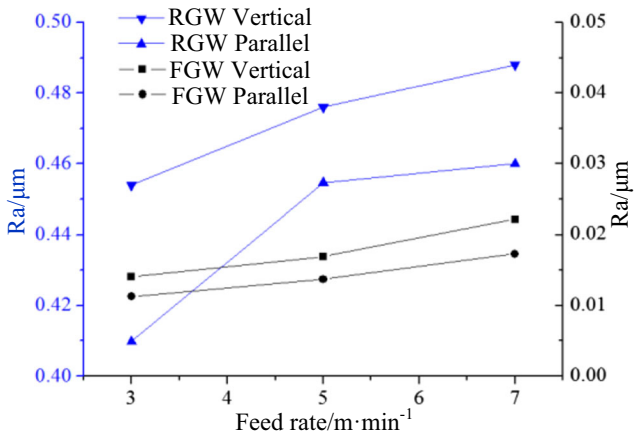

Fig. 6 Variation of SR with respect to feed rate

lateral crack depth; therefore, the relationship between SR and f_n is given by

$$\mathrm{SR} = 0.43(\sin\psi)^{1/2}(\cot\psi)^{1/3}\left(\frac{E}{H}\right)^{m}\left(\frac{f_n}{H}\right)^{1/2} \quad (2)$$

Where ψ is the sharpness angle of indenter, E is the elastic modulus, and H is the hardness.

As shown in Eq. 2, the value of SR is determined by material mechanical properties (elastic modulus and hardness), geometrical properties (sharpness angle), and average edge grinding force. Small average edge grinding force leads to small SR. For this reason, the values of SR in flexible grinding are much less than diamond grinding, in accordance with experimental results shown in Figs. 5 and 6.

3.4 Micrographs of grinding surface

Figure 7a–c illustrated the micrographs of FGW grinding surface (×1000) in condition of feed rate 5 m min^{-1} and grinding depth 10 and 20 μm. All these grinding surfaces have regular grinding trace. As shown in Fig. 7b, c, scallops generally increase both with deepening the grinding depth and increasing the feed rate, and the grinding depth has greater impact. Figure 7d shows the micrographs of the RGW grinding surface (×1000) in the condition of grinding depth 10 μm and feed rate 5 m min^{-1}. Compared to the FGW grinding surface, more grinding trace and scallops are obviously distributed on the RGW grinding surface. In addition, these results also verify that FGW grinding has advantage in controlling HSF errors.

3.5 Analysis of SSD

Table 3 shows the SSD depths of fused silica in flexible grinding and diamond grinding based on the computing model. Whatever the grinding mode takes, the SSD depths are directly proportional to the grinding depth and feed rate, but SSD

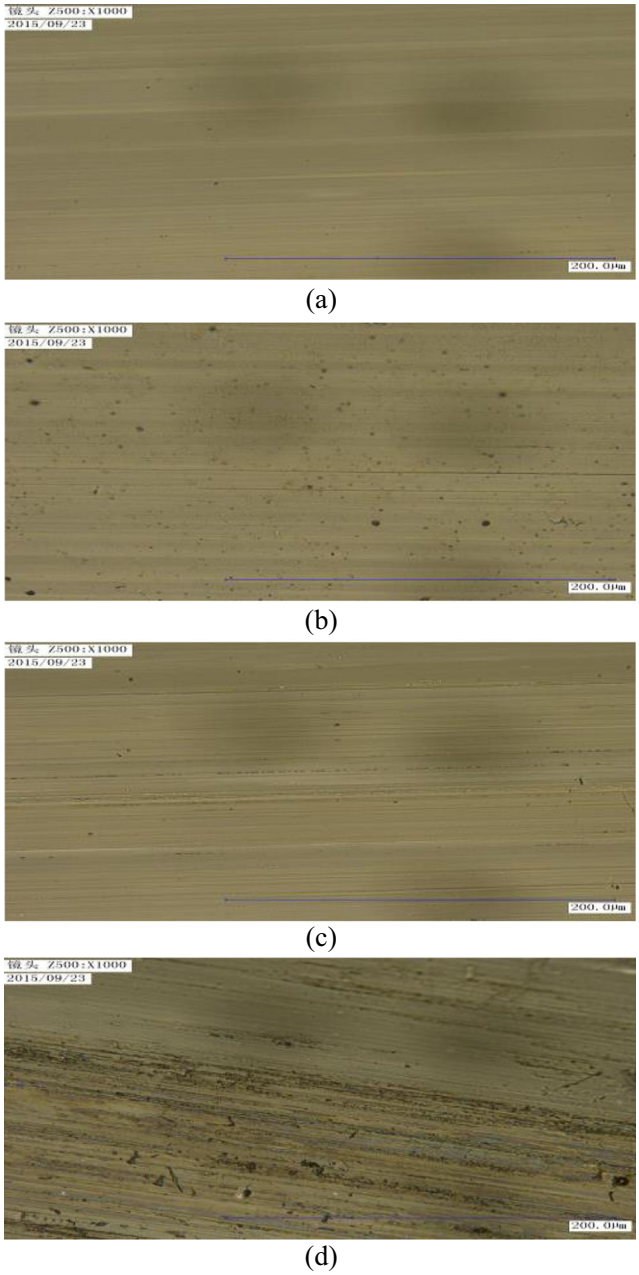

Fig. 7 Surface micrographs (×1000 magnification). **a** FGW, grinding depth = 10 μm, feed rate = 5 m min^{-1}. b FGW, grinding depth = 15 μm, feed rate = 5 m min^{-1}. **c** FGW, grinding depth = 10 μm, feed rate = 7 m min^{-1}. **d** RGW, grinding depth = 10 μm, feed rate = 5 m min^{-1}

Table 3 SSD depths of grinding fused silica

Grinding depth (μm)	Feed rate (m min^{-1})	SSD (RGW) (μm)	SSD (FGW) (μm)
10	5	29.3	2.2
15	5	35.5	2.9
10	3	26.4	1.6
10	7	32.9	2.3

depths of flexible grinding are much less than diamond grinding.

The Eq. 3 also proposed by Lambropoulos et al. [25] can explain why flexible grinding causes smaller SSD depths.

$$\mathrm{SSD} = {\alpha_k}^{2/3}\left(\frac{E}{H}\right)^{(1-m)2/3}(\cot\psi)^{4/9}\left(\frac{f_n}{K_c}\right)^{2/3} \quad (3)$$

where m is a dimensionless constant in the range $m = 1/3$ to $1/2$, K_c is the fracture toughness, and α_k is a dimensionless number given by $\alpha_k = 0.027 + 0.09(m - 1/3)$.

SSD depths are directly proportional to average edge grinding force. As discussed in Section 3.3, the average edge grinding force f_n in FGW grinding is less so that the values of SSD depth are smaller.

4 Conclusions

Based on the mechanism of FGW grinding and designing of FGW, surface errors and SSD in the flexible grinding of optical fused silica are discussed and the experiments are carried out. The surface errors, surface topography, and SSD are investigated. The results can be concluded as follows:

1. The LSF and HSF errors of optical fused silica after FGW grinding are much less than RGW grinding due to its precision and elastic characteristic. The influences of grinding parameters on surface errors and SSD in FGW grinding are the same as RGW grinding.
2. When comparing the optical fused silica surface micrographs of the two grinding modes, the surface quality of FGW grinding is much better.
3. Although FGW grinding cannot eliminate the MSF errors of optical fused silica thoroughly, it still can eliminate MSF errors within the range of PSD1.
4. The depths of SSD in FGW grinding are much less than the RGW grinding of optical fused silica.

Acknowledgements The first author would like to express his deep appreciation to Xiamen University for providing the experimental space and equipment. This work was supported by Xiamen University of Technology's high-tech project (YKJ14039R).

References

1. Brinksmeier E, Mutlugunes Y, Klocke F, Aurichc JC, Shored P, Ohmorie H (2010) Ultra-precision grinding. CIRP Ann Manuf Technol 59(2):652–671
2. Wang CC, Fang QH, Chen JB, Liu YW, Jin T (2016) Subsurface damage in high-speed grinding of brittle materials considering kinematic characteristics of the grinding process. Int J Adv Manuf Technol 83(5):937–948
3. Sayuti M, Ahmed AD, Fadzil M, Hamdi M (2012) Enhancement and verification of a machined surface quality for glass milling operation using CBN grinding tool-Tanuchi approach. Int J Adv Manuf Technol 60(9):939–950
4. Liu YM, Warkentin A, Bauer R, Gong YD (2013) Investigation of different grain shapes and dressing to predict surface roughness in grinding using kinematic simulations. Precis Eng 37(3):758–764
5. Tamkin JM, Milster TD (2010) Effects of structured mid-spatial frequency surface errors on image performance. Appl Opt 49(33): 6522–6536
6. Wang C, Yang W, Ye S, Wang ZZ, Yang P, Peng Y, Guo Y, Xu Q (2014) Restraint of tool path ripple based on the optimization of tool step size for sub-aperture deterministic polishing. Int J Adv Manuf Technol 75(9):1431–1438
7. Dong ZC, Cheng HB, Tam HY (2014) Further investigations on fixed abrasive diamond pellets used for diminishing mid-spatial frequency errors of optical mirrors. Appl Opt 53(3): 327–334
8. Suratwala T, Wong L, Miller P, Feit MD, Menapace J, Steele R, Davis P, Walmer D (2006) Sub-surface mechanical damage distributions during grinding of fused silica. J Non-Cryst Solids 352(52–54):5601–5617
9. Demir H, Gullu A, Ciftci I, Seker U (2010) An investigation into the influences of grain size and grinding parameters on surface roughness and grinding forces when grinding. J Mech Eng 56(7–8):447–454
10. Zhou XS, Li SY, Dai YF, Zheng ZW, Yang Z (2007) Correcting errors in definite area: a new method for controlling mid-spatial-frequency errors in optical surface. Opt Precis Eng 15(11):1668–1673
11. Tam HY, Cheng HB (2010) An investigation of the effects of the tool path on the removal of material in polishing. J Mater Process Technol 210(5):807–818
12. Dunn CR, Walker DD (2008) Pseudo-random tool paths for CNC sub-aperture polishing and other applications. Opt Express 16(23): 18942–18949
13. Li Y, Zheng N, Li H, Hou J, Lei X, Chen X, Yuan Z, Guo Z, Wang J, Guo Y, Xu Q (2011) Morphology and distribution of subsurface damage in optical fused silica parts: bound-abrasive grinding. Appl Surf Sci 257(6):2066–2073
14. Gu W, Yao Z, Li H (2011) Investigation of grinding modes in horizontal surface grinding of optical glass. J Mater Process Technol 211(10):1629–1636
15. Esmaeilzare A, Rahimi A, Rezaei SM (2014) Investigation of subsurface damage and surface roughness in grinding process of Zerodur glass-ceramic. Appl Surf Sci 313(7): 67–75
16. Chen JB, Fang QH, Li P (2015) Effect of grinding wheel spindle vibration on surface roughness and subsurface damage in brittle material grinding. Int J Mach Tools Manuf 91: 12–23
17. Bzymek ZM, Song G, Howes TD, Garrett RE (1994) Design of flexible grinding wheel with variable hub thickness. J Eng Ind 116(2):260–262
18. Guo YB, Yang ZS, Liang XC, Syoji K (2000) Study on a new type of soft wheel for high efficiency grinding. J Chongqing Univ(Nat Sci Ed) 23(1):9–11
19. Webster J, Tricard M (2004) Innovations in abrasive products for precision grinding. CIRP Ann Manuf Technol 53(2): 597–617
20. Zhou LB, Shimizu J, Kamiy S, Iwas H, Kimurac S, Satod H (2006) Defect-free fabrication for single crystal silicon substrate by chemo-mechanical grinding. CIRP Ann Manuf Technol 55(1):313–316

21. Lv DX, Huang YH, Tang YJ, Wang HX (2013) Relationship between subsurface damage and surface roughness of glass BK7 in rotary ultrasonic machining and conventional grinding processes. Int J Adv Manuf Technol 67(1):613–622
22. Hu CL, Bi G, Ye H, Li HY (2014) Research on detection of subsurface damage on grinding optical elements. J Synth Cryst 43(11): 2929–2934
23. Lin XH, Wang ZZ, Guo YB, Peng YF, Hu CL (2013) Research on the error analysis and compensation for the precision grinding of large aspheric mirror surface. Int J Adv Manuf Technol 71(1):233–239
24. Huang Y, Huang Z (2009) The modern abrasive belt grinding technology and engineering application. Chongqin University Press
25. Lambropoulos JC, Jacobs SD, Gillman BE, Stevens HJ (2005) Deterministic microgrinding, lapping and polishing of glass-ceramics. J Am Ceram Soc 88(5):1127–1132